

Modeling The Transition From Non-Sooting To Sooting, Coflow Ethylene Diffusion Flames

M. D. Smooke
Yale University, New Haven, CT

R. J. Hall
West Hartford, CT

M. B. Colket
United Tech Res Ctr, East Hartford, CT

Abstract

The transition from non-sooting towards sooting ethylene, coflow diffusion flames at atmospheric pressure has been studied previously as a function of fuel dilution by inert nitrogen. In our numerical simulations, predicted flame heights, temperatures, and acetylene are in good agreement with experiment. As ethylene dilution is decreased and soot levels increase, the experimental maxima in soot moves from the centerline toward the wings of the flame; similar trends are observed in the simulations. However, benzene simulations are significantly under predicted and soot concentrations are nearly always under predicted along the centerline of the flame. To resolve these issues, we have compared (i) more comprehensive chemical kinetics models and (ii) different soot formation/oxidation models. In addition, based on estimates of radiative heat transfer to the centerline of the burner, we preliminarily conclude treatment of such effects is an important requirement for modeling soot formation in these flames.

Introduction

Significant advancements in soot formation models have been made in the past ten years and these models have been applied to a range of complex combustion problems. Regardless of many apparent successes, there are few quantitative demonstrations in cases that include not only soot formation, but also its oxidation in non-premixed flames, for 2-d geometries and over a range of operating conditions. Modeling results have been presented for axisymmetric, coflow diffusion flames by others [1,2] as well as ourselves [3,4] for both methane and ethylene flames. Recently, we have been attempting to simulate sooting fields as measured in a series of ethylene coflow diffusion flames over a range of fuel dilution levels [5]. This contrast of some surprising successes in soot modeling against other failures observed when attempting to model a range of complex operating conditions highlights existing uncertainties and inaccuracies in modeling of soot emissions from flames. It is the objective of this work to identify some limitations of existing models and suggest alternative approaches. In an effort to increase understanding of these issues, we present here new results in which we compare simulations using one model over a range of conditions and contrast results from a combination of different chemical kinetic sets and soot formation models.

Results and Discussion

Data Used for Comparison

The experimental results to which the models are compared have been presented previously [4,5]. Atmospheric pressure, overventilated, axisymmetric, coflowing, nonpremixed laminar flames were generated with a burner in which the fuel flows from an uncooled 4.0 mm inner diameter vertical brass tube (wall thickness 0.38 mm). The oxidizer flows from the annular region between this tube and a 50 mm diameter concentric tube. The oxidizer was air while the fuel was a mixture containing ethylene and nitrogen. The fuel and oxidizer flow velocities are 35 cm/sec. The temperature of the brass tube for this slightly lifted flame was less than 330 K. In addition to the flame investigated in [4] with the central fuel tube feed with 32% ethylene and the remainder nitrogen, three additional flames were investigated by [5], with matched experimental inlet conditions except that the fuel dilution levels were changed to 40%, 60%, and 80% ethylene. Temperatures (corrected thermocouples), gas-phase species (microprobe sampling with mass spectrometric analysis), and soot volume fractions (LII and TPD) are available from these prior studies.

Description of the Flame Model

The axisymmetric computational model [3,4] employs the gas-phase diffusion flame equations in the velocity-vorticity formulation with buoyancy and the particle sectional approach presented in [6]. The result is a strongly coupled set of elliptic partial differential equations. The gas and soot equations are additionally coupled through non-adiabatic radiative loss in the optically-thin approximation. Radial and axial velocities, the vorticity, the temperature, the gas-phase species and the particle sectional mass fractions are computed. Details of the gas-phase kinetics and the soot models are described below. Twenty soot sections are included in the formulation. The system is closed with the ideal gas law and appropriate boundary conditions are applied on each side of the computational domain. Local properties are evaluated via transport and chemistry libraries. The sectional thermophoretic velocities in the free molecule regime are given in [6] as are the sectional diffusion velocities written with a mass-weighted mean diffusion coefficient for each size

class. The governing conservation equations are solved on a two-dimensional mesh by combining a Newton-based steady-state and a time-dependent solution method [7]. A time-dependent solution is first obtained on a coarse grid and then grid points are inserted adaptively to increase the resolution in regions of high spatial activity. In the optically thin approximation employed in this study, the power radiated from soot and gas bands (CO_2 , H_2O , and CO) is given by the volume integral given in [8]. An approximate uncoupled analysis to assess the importance of optical thickness was also performed in this work.

Kinetics and Soot Models

In this study, results from two kinetic models and two soot models are compared. The first kinetic model (SSWL) is modified (see below) from that developed by [9] and the second (FRK) is identical to that available from [10]. The largest species in the modified SSWL mechanism is benzene, whereas the FRK mechanism includes species to pyrene. The first soot model (HSC) is derived from [6], but with a revised inception model. The second soot model (FRS) is that available from [10], except that our sectional approach has been utilized for treatment of the aerosol dynamics. It is assumed that this difference will cause no significant differences in the predictions of soot volume fractions.

Since soot particles reach a maximum primary size in experiments, the model ceases both coalescence and surface growth above a preset particle size. In the HSC model, particle surface growth is truncated at a specified primary particle diameter (in these calculations 31 nm) to simulate the effects of particle ageing. In all the model calculations, particle coalescence is similarly truncated at a specified particle diameter to simulate the appearance of fractal aggregates of primary particles. In general, the sectional analysis is not limited to spherical particles; adding equations for the average number of primary spheroids within a section enables modeling formation of soot aggregates, as well [11,12].

Soot inception in this HSC model builds upon our earlier formulation [6] of naphthalene production rates. Quasi steady-state concentrations of intermediate polycyclic aromatic hydrocarbons are assumed to exist and attained rapidly. In this proposed model, instead of the presumption that naphthalene and phenanthrene lead directly to inception, steady-state expressions have been derived for the formation of a high molecular weight condensed polycyclic aromatic hydrocarbon (PAH). The model is based on the sequence of growing naphthalenyl to pyrenyl through sequential acetylene addition, H-atom elimination, H-atom abstraction, acetylene addition followed by ring closure. Limitations to the use of this expression are related to (1) uncertainties in the side reactions that may remove critical intermediate species and (2) the time it takes to achieve steady-state concentration levels. The big benefit is that this approach eliminates the need for detailed modeling of the higher order polycyclic aromatic hydrocarbons, which is still uncertain. Utilization of this approximate reaction sequence for inception prevents coalescence for very small particle sizes.

Transition to Sooting Flames using Model A

The majority of the computations have been performed utilizing the modified SSWL kinetics and the HSC soot model. The model set is referred here to Model A. Two other sets of computations were also performed. Model B is based upon the larger kinetics set, FRK, which is coupled to the HSC soot model. Model C utilizes the FRK kinetics and the FRS soot model. Figure 1 shows temperature (Model A) as a function of height, along the centerline for the four flames in this study. As concluded previously [4], the high experimental temperatures very low in the flame (< 1 cm) are likely a result of limitations in the experimental method at these locations. The model does a very good job of reproducing the rapid rise in temperature at heights of 1.0-2.5 cm; but the computations do not adequately approach nor attain the peak centerline temperatures. Also shown in Fig. 1 is the centerline profile for the 80% ethylene case in which radiation is ignored. Non-adiabatic radiative loss drastically modifies the temperature profile, and lengthens the flame by about 15%. Losses are primarily due to gas-band radiation, although loss due to continuum radiation from soot particles becomes increasingly important with increasing soot volume fractions and at higher heights in the flame. Comparison of the computed temperature with experimental data suggests that we may be overestimating radiation losses.

Acetylene is a principal surface growth species and also contributes to inception. Hence, accurate simulation of acetylene is also critical to predictions of soot. Acetylene profiles are simulated well and the changes with decreasing dilution are also reproduced, although concentrations are under predicted at low heights. The model for the 32% ethylene flame reproduces benzene concentrations along the centerline reasonably, but significant increases in benzene observed experimentally with decreasing dilution are not simulated well and are spatially displaced. The under prediction of benzene (trend with increasing fuel concentration) can be expected to affect predicted soot concentrations. Presumably, these low benzene predictions are directly linked to the low temperature predictions in this portion of the flame. The under predicted temperatures may inhibit faster growth rates lower in the flame and under predict rapid thermal decomposition rates higher in the flame. The dramatic changes in the benzene and acetylene profiles, when radiation losses are not included demonstrate this dependency.

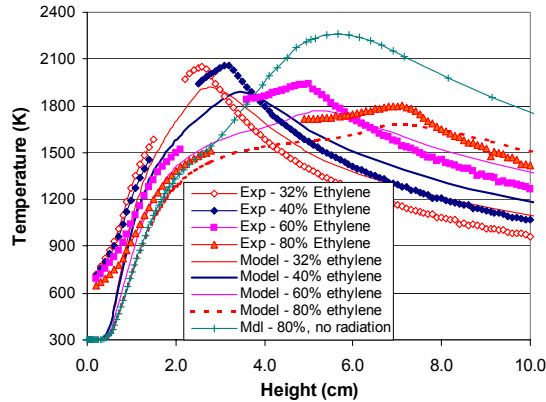


Figure 1. Comparison of Predicted and Experimental Centerline Temperatures as a Function of Height for diluted Ethylene Flames. (Radiation-Free solution for the 80% flame is included.)

Experimental soot volume fractions for the 32%, 40%, 60% and 80% flames are compared to the computed solutions (Model A). The experiments depict a dramatic shift in the location of maximum soot away from the centerline to the wings as ethylene is increased. This trend is identical to that reported by Santoro and coworkers [13] with increasing fuel flow rate nearly 20 years ago. The model, though it under predicts the peak soot levels, agrees qualitatively with this trend. The dilute flame has a temperature profile that peaks on the centerline, with soot forming below the flame front and peaking on the centerline. As the ethylene flow increases, the temperature peaks off the centerline; soot will be formed inside the flame front and grow along the full length of the flame, confined by thermophoretic force. Thus, as the flame lengthens with decreased levels of dilution, soot levels in the wings increase substantially due both to the increased residence time and to the increased levels of (experimental) benzene. As discussed previously, uncertainties in the predictions of benzene and temperature contribute to inaccuracies in the quantitative prediction of soot along the centerline with decreasing dilution of the fuel, but the qualitative trend is predicted.

Comparison of Models for 60% Ethylene Flame

In an effort to examine the effects of the gas-phase kinetics model and the soot model, calculations were performed for the 60% ethylene flame with Models B and C. These newer results are compared in Table I to the experimental data and to the Model A computations. Generally, predicted species concentrations were nearly identical for the two kinetic mechanisms (SSWL – Model A and FRK – Models B and C), but predicted benzene concentrations with the FRK mechanism are lower and peak slightly lower in the flame (but still somewhat higher than the experimental data).

Note that Model B provides a f_v field nearly identical to that from Model A despite the different kinetics sets. The magnitude of the predicted f_v with Model B are lower, presumably due to the lower benzene predictions with this kinetic set. Predictions with Model C peak along the centerline. An analysis of the relative difference indicates that the relative contribution to soot mass growth from pyrene (due to inception and surface growth) in the FRS model is much higher than the inception rate as simulated by the HSC model. Hence, soot concentrations peak along the centerline for the FRS model. One can anticipate that once the temperature field and benzene profiles are simulated properly, the models will all predict higher levels of inception and growth along the centerline.

While differences between the models are apparent, final conclusions regarding the suitability of either model should be made after simulations are made that include the scrubbing effects. Ideally, such simulations can be performed using a flame model that predicts better the flame temperatures along the centerline and the aromatic concentrations.

Conclusions

Laminar, sooting, ethylene-fueled, coflow diffusion flames have been studied theoretically as a function of ethylene dilution. Flame parameters important to prediction of soot concentrations have been measured, and thus the experiments pose a very stringent test for assessment of chemical and soot kinetics mechanisms. Predicted flame heights, temperatures, and acetylene are in excellent to good agreement with experiment. Experimentally, soot profiles obtained from laser-induced soot incandescence (LII) undergo a shift away from peaking on the flame centerline toward the wings of the flame as the sooting level increases. Theoretical simulations agree qualitatively with this observation. Modifications to the soot model have been tested. The most effective were (i) termination of surface growth and

coalescence at a predetermined diameter (e.g., about 25 nm), (ii) use of a more comprehensive reaction model, and (iii) simulation of large molecular weight PAHs for inception. Agreement with the experimental data set is again good, although centerline temperatures, benzene concentrations and soot volume fractions are progressively under predicted as dilution levels decrease. Comparison of the kinetics/soot models demonstrates the variability in benzene predictions and the relative contributions of inception and surface growth due to various modeling approaches.

Table I. Comparison of Model Predictions for the 60% Ethylene Coflow Flame

	Exp	Mdl A	Mdl B	Mdl C
Flame Height (cm)	5.0	5.2	5.2	4.7
Pk Temp (K)	2199	2054	2027	2057
Peak CL Temp (K)	1970	1765	1716	2014
Peak Soot (ppm)	6.0	4.3	4.0	0.75
Pk CL Soot /Pk Soot	0.59	0.48	0.38	1.00
Pk Acetylene (%)	4.3	4.4	4.75	5.12
Pk Benzene (ppm)	630	359	263	297

Acknowledgements

The authors acknowledge support from the Air Force Office of Scientific Research (Dr. Julian Tishkoff, contract monitor) and the DOE Office of Basic Energy Sciences (Dr. Paul Maupin, contract monitor) for support of this work under contracts F49620-98-C-0008 and DE-FG02-88ER13966, respectively. We are also grateful to Mr. Brian Dobbins for his assistance in the preparation of the figures.

References

- Kennedy, I.M., Rapp, D.R., Santoro, R.J., and Yam, C., *Combust. Flame*, 107:386, (1996).
- Kaplan, C.R., Shaddix, C.R., and Smyth, K.C., *Combust. Flame*, 106:392, (1996).
- Smooke, M. D., McEnally, C. S., Pfefferle, L. D., Hall, R. J. and Colket, M. B., *Combust. and Flame*, 117:117, (1997).
- McEnally, C. S., Schaffer, A. M., Long, M. B., Pfefferle, L. D., Smooke, M. D., Colket, M. B., and Hall, R. J., *Proceedings of the Combustion Institute*, 27, The Combustion Institute, p. 1497, (1998).
- Smooke, M. D., McEnally, C. S., Fielding, J., Long, M. B., Pfefferle, L. D., Hall, R. J., and Colket, M. B., "Investigation of the Transition from Non-Sooting Towards Sooting, Coflow Ethylene Diffusion Flames", *Proceedings of the Second Joint Meeting of the U.S. Sections of The Combustion Institute*, Oakland, CA, March 25-28, 2001.
- Hall, R.J., Smooke, M.D., and Colket, M.B., in *Physical and Chemical Aspects of Combustion: A Tribute to Irvin Glassman*, ed. by R.F. Sawyer and F.L. Dryer, Combustion Science and Technology Book Series, Gordon and Breach, (1997).
- Smooke, M.D., Ern, A., Tanoff, M.A., Valdati, B.A., Mohammed, R.K., Marran, D.F. and Long, M.B., *Proceedings of the Combustion Institute*, 26, The Combustion Institute, p. 2161, (1996).
- Hall, R.J., *JQSRT*, 51:635, (1994).
- Sun, Sung, Wang, H., and Law, C.K., *Combust. and Flame*, 107:321 (1996). A copy of the modified mechanism is available on request (colketmb@utrc.utc.com)
- Appel, J., Bockhorn, H. and Frenklach, M.Y., *Combust. Flame*, 121:122-136 (2000). Avail from <http://www.me.berkeley.edu/soot/mechanisms/mechanisms.html>
- Rogak, S.N., PhD Dissertation, Cal. Tech., (1991).
- Rogak, S.N., *Aerosol Science and Technology*, 26: 127 (1997).
- Santoro, R. J., Semerjian, H. G., and Dobbins, R. A., *Combust. Flame*, 51:203, (1983).

In combustion, a diffusion flame is a flame in which the oxidizer and fuel are separated before burning. Contrary to its name, a diffusion flame involves both diffusion and convection processes. The name diffusion flame was first suggested by S.P. Burke and T.E.W. Schumann in 1928, to differentiate from premixed flame where fuel and oxidizer are premixed prior to burning. The diffusion flame is also referred to as nonpremixed flame. The burning rate is however still limited by the rate of diffusion. This paper represents a systematic investigation on the best model predicts the temperature and soot production in coflow jet flame, by applying various RANS turbulent model, soot models and radiation models in presence or absence of gravity. It also applies this model predicted in crossflow jet flame and investigates the velocity ratio (ratio of the velocity of fuel jet to the velocity of air stream) variation effect on temperature and soot production. Figure 2 : Diagram of gas turbine jet engine [9]. Non-premixed flames are also called diffusion flames because the reacting species have to reach the flame front before reaction by molecular diffusion. They are exposed to turbulence and diffusion speeds when they travel and can be strongly modified by the turbulence motions. Two axisymmetric laminar coflow non-smoking and smoking ethylene diffusion flames are studied numerically in order to assess the influence of different radiative property models on the soot formation and oxidation processes. Simulations are carried out by considering the Steady Laminar Flamelet (SLF) concept and a modified two-equation acetylene-based model to describe the soot nucleation, [Show full abstract] surface growth and oxidation processes. Several radiative property models are considered: the simple Optically Thin Approximation (OTA), the Weighted-Sum of Grey-Gases (WSGG), the Gr Laminar, sooting, ethylene-fueled, coflow diffusion flames at atmospheric pressure have been studied experimentally and theoretically as a function of fuel dilu... The transition from non-sooting to sooting coflow ethylene diffusion flames. DOI: 10.1615/ICHMT.2004.CHT-04.110 page 11. Computations are also presented for modifications to the model that include: (i) a revised inception model; (ii) a maximum size limit to the primary particle size and (iii) estimates of radiative optical thickness corrections to computed flame temperatures. Purchase \$25.00 Check subscription Download MARC record Editorial Board Publication Ethics and Malpractice Recommend to my Librarian Bookmark this Page.